Science of the Total Environment 823 (2022) 153705

Contents lists available at ScienceDirect

Science of the Total Environment

journal homepage: www.elsevier.com/locate/scitotenv

Stormwater management in urban areas using dry gallery infiltration systems

Miguel Ángel Marazuela [a,*], Alejandro García-Gil [b], Juan C. Santamarta [c], Samanta Gasco-Cavero [b], Noelia Cruz-Pérez [c], Thilo Hofmann [a]

[a] Centre for Microbiology and Environmental Systems Science, Department of Environmental Geosciences, University of Vienna, Althanstrasse 14 UZAII, 1090 Vienna, Austria
[b] Geological Survey of Spain (IGME-CSIC), C/Ríos Rosas 23, 28003 Madrid, Spain
[c] Agriculture, Nautical, Civil and Maritime Engineering Department. University of La Laguna (ULL), Ctra. Geneto, 2, La Laguna, 38200 Tenerife, Canary Islands, Spain

HIGHLIGHTS

- *Dry galleries* as novel stormwater infiltration facilities are presented.
- A 3D unsaturated flow model considering different geological settings is performed.
- Layering of volcanic aquifers strongly constrains infiltration performance.
- Sizing errors of 100% occur neglecting unsaturated conditions.
- Installation and management guidelines for dry galleries are provided.

GRAPHICAL ABSTRACT

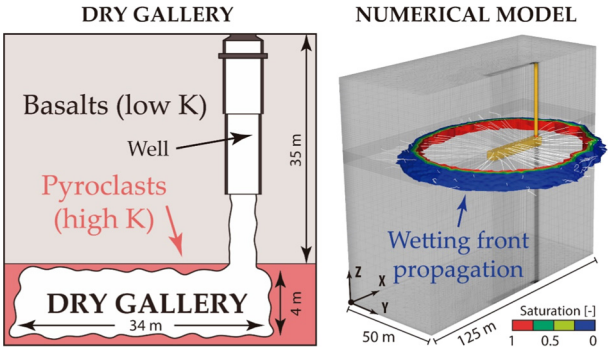

ARTICLE INFO

Article history:
Received 20 December 2021
Received in revised form 2 February 2022
Accepted 2 February 2022
Available online 5 February 2022

Editor: Damià Barceló

Keywords:
Unsaturated flow
Vadose zone
Numerical model
Volcanic aquifer
Artificial recharge
Managed aquifer recharge

ABSTRACT

The increase in the frequency of extreme precipitation events due to climate change, together with the continuous development of cities and surface sealing that hinder water infiltration into the subsoil, is accelerating the search for new facilities to manage stormwater. The Canary Islands (Spain) are taking advantage of the knowledge acquired in the construction of water mines to exploit a novel stormwater management facility, which we have defined as a *dry gallery*. Dry galleries are constituted by a vertical well connected to a horizontal gallery dug into highly permeable volcanic layers of the vadose zone, from where infiltration takes place. However, the lack of scientific knowledge about these facilities prevents them from being properly dimensioned and managed. In this work, we simulate for the first time the infiltration process and the wetting front propagation from dry galleries based on a 3D unsaturated flow model and provide some recommendations for the installation and sizing of these facilities. The fastest advance of the wetting front takes place during the earliest times of infiltration (<2 h), with plausible propagation velocities and infiltration rates higher than 1000 $m \cdot d^{-1}$ and 2 $m^3 \cdot s^{-1}$. As time progresses, the propagation velocity and infiltration rate decrease as a consequence of the hydraulic gradient attenuation between the gallery and the aquifer. Therefore, stormwater infiltration is a highly transient process in which a sizing underestimation of 100% may be committed if unsaturated conditions or geological configuration are neglected.

1. Introduction

Climate change is increasing the frequency of extreme precipitation events at the same time that cities are gaining more and more ground from land surface, significantly reducing the infiltration capacity of the

* Corresponding author.
E-mail address: miguel.angel.marazuela@univie.ac.at (M.Á. Marazuela).

http://dx.doi.org/10.1016/j.scitotenv.2022.153705

soil (Allen and Ingram, 2002; Berg et al., 2013; Fischer and Knutti, 2016; Fischer and Knutti, 2015; Myhre et al., 2019; Pfahl et al., 2017; Vázquez-Suñé et al., 2016). Precipitation that would normally reach natural land surface and infiltrate into the underlying aquifer instead runs off, traveling over paved areas until it evaporates or enters stormwater management facilities (Clark and Pitt, 2007). This problem becomes even more important in island populations, where the scarcity of water resources is an almost global issue (Gössling, 2001; Papapostolou et al., 2020).

One of the most outstanding examples of the necessity for efficient water resources management is the Canary Island archipelago (Spain) (Custodio et al., 2016; Custodio et al., 2015), which holds 2.2 million inhabitants and received more than 15 million tourist visitors in 2019 (Hernández-Martín et al., 2021). The strong urban development of the Canary Islands and the waterproofing of its land surface is leading buildings and urbanization resorts to the installation of stormwater infiltration facilities in the last decade.

Although commonly built to control stormwater, infiltration facilities are also used for managed artificial recharge (MAR) of aquifers in areas with scarcity of water, so they are frequently studied and classified together. These facilities can be split into three subcategories: surface infiltration systems (e.g., MAR ponds), vadose infiltration systems (e.g., drywells, infiltration galleries) and injection wells. Each one of them has a very different design, installation depth with respect to the land surface and operational performance, as many previous works have addressed (e.g., Bouwer, 2002; Dillon, 2005; Edwards et al., 2016; Zhang et al., 2020). However, to our knowledge, there is no scientific reference whatsoever to galleries excavated in consolidated volcanic rocks operating in the vadose zone as infiltration facilities, here referred to as *dry galleries*. It is important not to confuse them with infiltration galleries, which are essentially covered percolation trenches (a few decimetres from the surface and often filled by unconsolidated materials) that contain a medium or supporting structure with internal void spaces to facilitate infiltration (Bekele et al., 2013).

Dry galleries are stormwater infiltration facilities composed of a vertical well (1–2 m of diameter) that connects with a horizontal gallery (often 5–50 m long and 2–5 m wide) dug by hand into layers of consolidated permeable rocks within the vadose zone from where stormwater infiltration is produced (Fig. 1). The gallery can be located at any depth within the unsaturated zone, although it is generally between 5 and 50 m deep. The design of the dry galleries is justified by the characteristic geological configuration of volcanic rocks where layers of impermeable rocks (e.g., basaltic rocks) alternate with others much more permeable (e.g., loosely packaged pyroclasts). The presence of impermeable layers with great lateral continuity between the surface and the water table would hinder infiltration from the surface through MAR ponds or infiltration galleries, while the relatively low thickness of the permeable layers (often below 5 m) notably limit the performance of drywells (Sasidharan et al., 2019). Local people know the importance of this layered geological configuration for extracting water from water mines (Custodio et al., 2016; Custodio et al., 2015; Custodio et al., 1983; Marrero-Diaz et al., 2015). Nowadays, due to the need to manage stormwater, dry galleries are increasingly being built in the last decade in the Canary Islands as instruments to infiltrate stormwater into the vadose zone. These systems are used in many urbanizations and constructions in the Canary Islands and, in many cases, their existence is unknown because they are still being regulated.

In the Canary Islands and many other parts of the world, the processing of authorization expedients for the stormwater spill in the vadose zone through infiltration facilities is still scarce, largely due to fear of wrong installation or management that could lead to polluting aquifers or damaging ecosystems. This is often accentuated by a lack of regulations that ensure

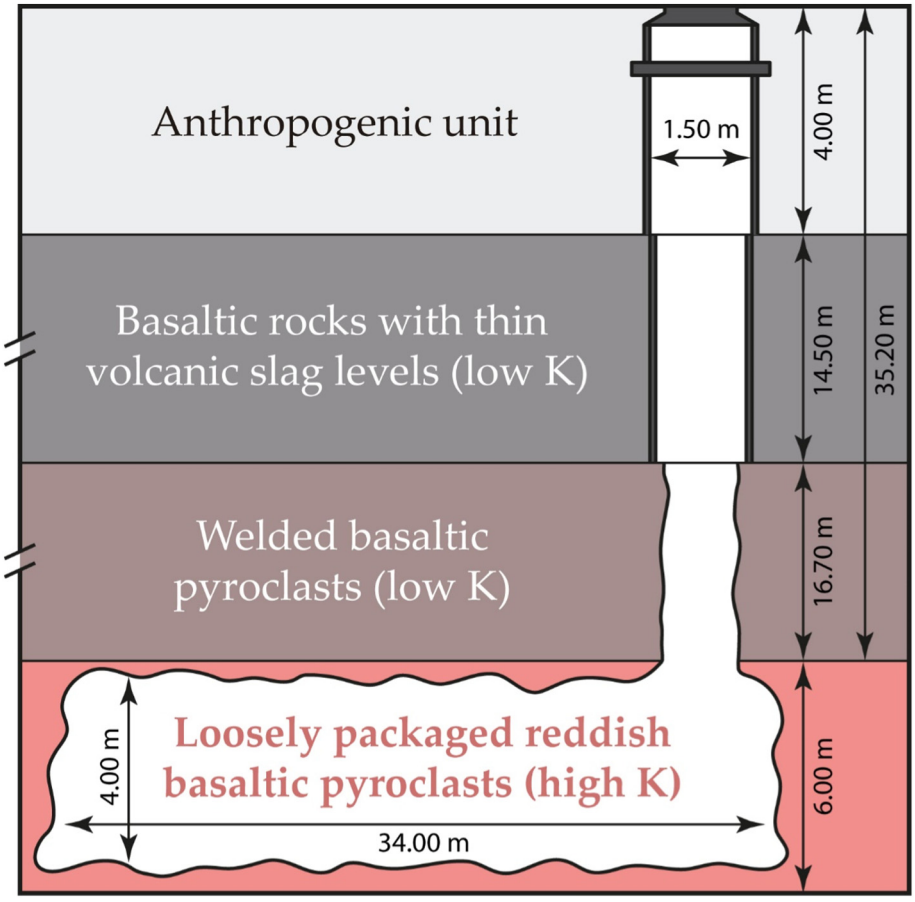

Fig. 1. Graphical representation of a dry gallery stormwater infiltration facility based on the *Santa Cruz* case study. Note the location of the dry gallery in the reddish basaltic pyroclasts of high hydraulic conductivity (K). Scale is not consistent in order to show all items in greater detail.

the quality of groundwater resources and the management of stormwater (Custodio et al., 2015). A poorly dimensioned infiltration device could have environmental consequences in addition to material damage to nearby infrastructure. Contaminants reaching the water table beneath inland areas can be transported by regional groundwater flow to near the coast, where groundwater flow rises and discharges into the sea, constrained by the saline interface (Folch et al., 2020; Izuka, 2011; Luijendijk et al., 2020; Marazuela et al., 2018; Martínez-Pérez et al., 2022). Also the contaminated water could be captured by extraction wells before reaching the coast, which could be risky in the case of drinking water. Although contaminants are linked to stormwater, especially those linked to particulate and increased turbidity and washed away by the first falling waters during rain events, the conclusion of the majority of studies is that when sizing is conducted properly, managed infiltration of stormwater does not pose a threat to groundwater and drinking water resources (Barraud et al., 1999; Dallman and Spongberg, 2012; Edwards et al., 2016). In this respect, a correct estimation of the travel time of the wetting front that is propagated through the vadose zone from infiltration systems toward the water table due to stormwater infiltration, together with correct sizing of the facility, is key.

Sizing guides have been made for other MAR systems such as drywells, based on experimental data and numerical simulations and in the field with very specific designs with defined geometries (Massmann, 2004). There are also some simplified analytical solutions for seepage trenches and ponds (Akan, 2002). Research dedicated to infiltration efficiency from other MAR systems has been carried out based on experiments and numerical model simulations (Bekele et al., 2013; Edwards et al., 2016; Sasidharan et al., 2019; Sasidharan et al., 2018). Even so, there are several works addressing drywells in continental locations but only a few of them in volcanic islands. Numerical contaminant transport modeling and general recommendations about drywell usage on the island of Hawaii was done by Izuka (2011). In the island of Hawaii, hydraulic conductivities (K) of up to 1000 m·day^{-1} was described along some permeable layers, as occurs in the Canary Islands. However, so far, no work has addressed the infiltration process from dry galleries drilled into consolidated volcanic rocks, nor have guidelines been proposed for its installation and management.

The fact that dry galleries are located in the unsaturated zone means the infiltration process becomes more complex (Gray and Hassanizadeh, 1991a, 1991b; Kool et al., 1987; Stephens, 1996). In unsaturated materials, the water content is less than the effective porosity, and the water pressure in pores is negative, being for a certain point less than the one that would correspond to that same point if the aquifer were completely saturated. This leads to higher hydraulic gradients than expected. Also, the layered disposition of the Canary Islands, and volcanic rocks in general, represents an additional element of complexity for quantification of the infiltration rate and then for the design and sizing of dry galleries. However, the groundwater flow modeling in the unsaturated zone requires a greater knowledge of the hydraulic parameters of the terrain and a higher computational cost (especially in 3D models) (Herrera et al., 2022; van Genuchten, 1980), which frequently leads to unsaturated conditions being left out in dry gallery sizing assessments. For these reasons, most geotechnical studies carried out so far in the Canary Islands assumed (i) flow in a saturated medium (K dependence to saturation is neglected), (ii) steady-state flow regime, (iii) hydraulic gradient equals to 1 (unit gradient) on the floor, walls and ceiling of galleries and (iv) homogeneous and isotropic K field (IGME, 2021). The assumption of all these simplifications seems to be excessively simplistic but the reality is that there are no effective analytical models to reproduce the infiltration from these infiltration facilities to assess the error committed. Also, permeability estimations might be imprecise, depending on the method chosen (e.g., Gilg-Gavard, Haefeli and Lefranc tests or borehole permeameter), the number of tests carried out and the application limitations for the unsaturated zone (Dezert et al., 2019; Elrick et al., 1989; Kindred and Reynolds, 2020; Lefranc, 1937; Lefranc, 1936; Stephens, 1992; Stephens, 1979; Stephens et al., 1987). An inadequate estimation of permeability can lead to overestimating the travel times of a potential pollutant existing in the gallery until it reaches the water table, reducing the pollutant attenuation time and putting water resources at risk. Thus, the need to generate a simplified reference model that addresses, from a numerical point of view, the transient infiltration process in dry galleries under layered and non-layered geological configurations and provides guidelines based on scientific criteria for the sizing and management of these facilities is evident.

This paper elucidates existing dry galleries of the Canary Islands which are being used as an effective stormwater infiltration facility but are mainly unknown to the scientific community. The objectives of this paper are (i) to evaluate, under isotropic and layered geological configurations, the geometry and velocity propagation of the wetting front triggered by the stormwater infiltration from dry galleries, (ii) the evolution of the infiltration performance over time and (iii) the errors made in dry gallery sizing by neglecting unsaturated conditions, with the purpose of providing scientifically based guidelines for the management of these facilities. To simulate the infiltration process through the unsaturated zone under different geological configurations from this novel stormwater infiltration facility, a synthetic 3D numerical model, based on the *Santa Cruz* dry gallery, was carried out. This dry gallery can be considered, due to its design and dimensions, as a first reference example for this new type of MAR system. The results of this study aim to guide stormwater management in other parts of the world, specially, in places where the layered geological configuration of rocks reduces the performance of other MAR systems.

2. The Canary Islands

The Canary Islands is a volcanic archipelago located on the African plate and constituted by seven islands, one minor island and several small islets covering an area of approximately 7500 km^2 (Fig. 2). The archipelago is located 1400 km from the Iberian Peninsula and 100 km from the African coast. The island of Tenerife, in the center of the Canary archipelago, is the largest, with an area of 2034 km^2. Its highest elevation is the Teide Peak, which reaches 3718 m a.s.l. (meters above sea level). Although the Canary Islands would have a dry and warm climate due to its latitude, the presence of the trade winds gives the northern slopes of the highest islands, such as Tenerife, a humid and temperate climate and comparatively drier southern slopes. The island receives an average annual precipitation of 420 mm. In the island of Tenerife, surface runoff water is hardly represented in the water supply, and groundwater coming from the recharge by precipitation provides almost 90% of drinking water (Santamarta-Cerezal et al., 2013).

From a geological point of view, the archipelago of the Canary Islands is mainly constituted by basaltic rocks generated from magma emissions from the Miocene to the present day. The Canary islands emerged from hotspots associated with a residual thermal plume, which has been active since the beginning of the Atlantic Ocean opening, 200 million years ago (Anguita and Hernán, 2000). The volcanism of the Canary Islands corresponds to the alkaline series, in which basalts, trachytes and phonolites predominate. Although different stratigraphic units emerge on the surface, the most modern series occupy most of the island's surface. Given their favorable primary characters and their low degree of compaction and alteration, these modern materials (pyroclasts, unwelded ignimbrites and breccias) are highly permeable (>100 m·day^{-1}) (IGME, 2021; Santamarta-Cerezal et al., 2013). The volcanic materials that make up the island are permeable by porosity and also cracking. By contrast, the old core materials are characterized by low hydraulic conductivities (<1 m·day^{-1}). The layered nature of volcanic rocks gives rise to a wide range of K values, ranging from 0.01 m·d^{-1} for ancient basalts and welded pyroclastic layers to more than 1000 m·d^{-1} in some recent quaternary basalts or loosely packaged pyroclasts. Also, porosity can range between almost 0% to more than 60%, although the pores do not always have good connectivity (Santamarta-Cerezal et al., 2013).

The insular hydrogeological functioning is characterized by the existence of a heterogeneous and anisotropic multilayer single aquifer (insular aquifer) on each island, with radial flow from the center of the island toward the coast or toward the deepest radial ravines. Rainwater infiltrates the permeable surface materials (lavas and pyroclasts) and descends

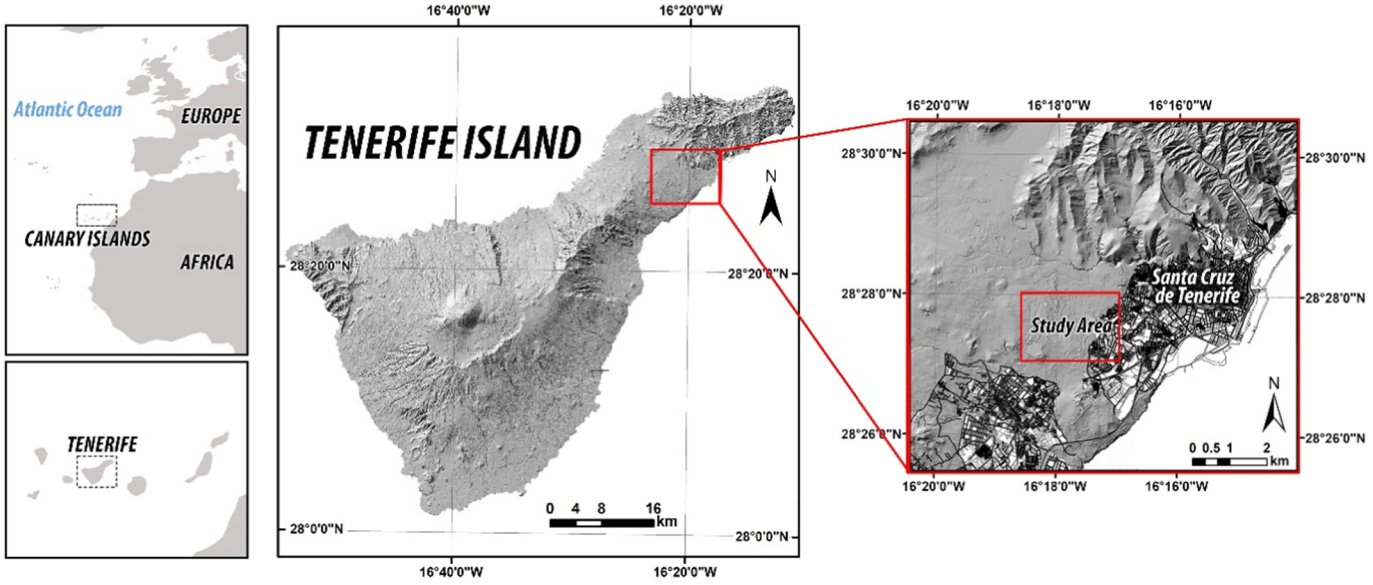

Fig. 2. Location of the investigated *Santa Cruz* dry gallery on Tenerife Island of the Canary Islands.

through the holes in the rocks until all of them are fully saturated, forming the main aquifer. Some of the high permeable layers are horizontally dug from the hillside and then used as water mines by locals (Custodio et al., 2016). In addition, there are some local hanging aquifers above this main aquifer, conditioned by poorly permeable layers, from which water percolates to deeper levels or discharge through small springs.

3. Material and methods

3.1. "Santa Cruz" dry gallery

The *Santa Cruz* dry gallery is located in the southeast of the island of Tenerife (San Cristóbal de La Laguna, Spain) and serves an urbanization with an area of 175,000 m^2 (Figs. 1 and 2). The *Santa Cruz* dry gallery is constituted by a vertical well of 35.2 m depth connected to a horizontal gallery 34 m long (IGME, 2021). The vertical well has a diameter of 1 m and is cased with blind pipe. The horizontal gallery has a rectangular prism shape with an average of 4 m width and height and a total infiltration surface area of 595 m^2. The infiltration gallery is located 35.2 m depth from the surface, which is at 420 m a.s.l. The scarcity of piezometric data led to the assumption that the water table is close to the sea level because of its proximity to the coast. In consequence, the thickness of the unsaturated zone was estimated at approximately 400 m. The water poured into the dry gallery is previously circulated through a sand trap to remove the potentially polluting particles of greater diameter.

The rocks of the top 35.2 m were defined as massive basalts and welded pyroclasts of very low K, with some anthropogenic detrital material at the top (Fig. 1). Underlying these massive basalts, where the dry gallery was dug, reddish basaltic pyroclasts of high K (140 $m{\cdot}day^{-1}$, according to the Haefeli test results) were found (IGME, 2021).

3.2. Numerical model set-up

A synthetic 3D transient-state unsaturated flow model based on the *Santa Cruz* dry gallery was developed with the FEFLOW code to simulate the groundwater flow under variable saturation conditions in the vadose zone associated with dry galleries. The basic equation for 3D flow in variably saturated porous media can be written in terms of the hydraulic head variable $h = \psi + z$ as (Diersch, 2014):

$$sS_0\frac{\partial h}{\partial t} + \varepsilon\frac{\partial s}{\partial t} + \nabla\cdot\mathbf{q} = Q \tag{1}$$

defining:

$$\mathbf{q} = -K_r\mathbf{K}\cdot\nabla h \tag{2}$$

where s is the saturation of fluid in the void space ε (effective porosity), S_0 is the specific storage coefficient, t is time, **q** is the Darcy velocity of fluid, **K** is the tensor of hydraulic conductivity, Q is the bulk source/sink term of flow, K_r is the relative hydraulic conductivity and z is the elevation head.

In addition, the following van Genuchten-Mualem parametric model is used for the present study (van Genuchten, 1980):

$$s_e = \begin{cases} \dfrac{1}{\left[1+|\alpha\psi|^n\right]^m} & \text{for } \psi < \psi_a \\ 1 & \text{for } \psi \geq \psi_a \end{cases} \tag{3}$$

$$K_r = s_e^{1/2}\left\{1-\left[1-s_e^{1/m}\right]^m\right\}^2 \tag{4}$$

where α, n and m are empirical parameters, ψ is the pressure head and s_e is effective saturation, generally defined as:

$$s_e = \frac{s-s_r}{s_s-s_r} \tag{5}$$

where s_r is residual saturation and s_s is maximum saturation.

The 3D numerical model comprised a domain of 125 m long, 100 m wide and 109.6 m high (Fig. 3A). It comprised 121 layers that decrease in thickness from 3 m to 0.1 m toward the horizontal gallery and $2.4{\cdot}10^6$ elements. The size of the elements ranged between 0.1 and 5 m. The top elevation of the model was 420 m a.s.l. The dry gallery of 34 m long and 4 m high and wide was located in a central position of the domain, 35.2 m beneath the top of the model and 70 m above the bottom. The filtering surface corresponding to the infiltration gallery was 576 m^2. The well that connected the surface with the dry gallery was at 35.2 m depth.

The model considered an initial condition in which the dry gallery and the well are completely filled with water, just before causing overflow. It is understood that once the stormwater infiltration device is filled to the surface (level 420 m), that will be the hydraulic head in the entire cavity and then this value was set as the initial and prescribed boundary condition. The hydraulic head inside the gallery remained at its maximum level (420 m a.s.l. or 39.2 m in terms of equivalent height of water column) during the entire simulation. The external boundaries of the domain were set as no-flow boundary conditions. However, as the wetting front never reaches

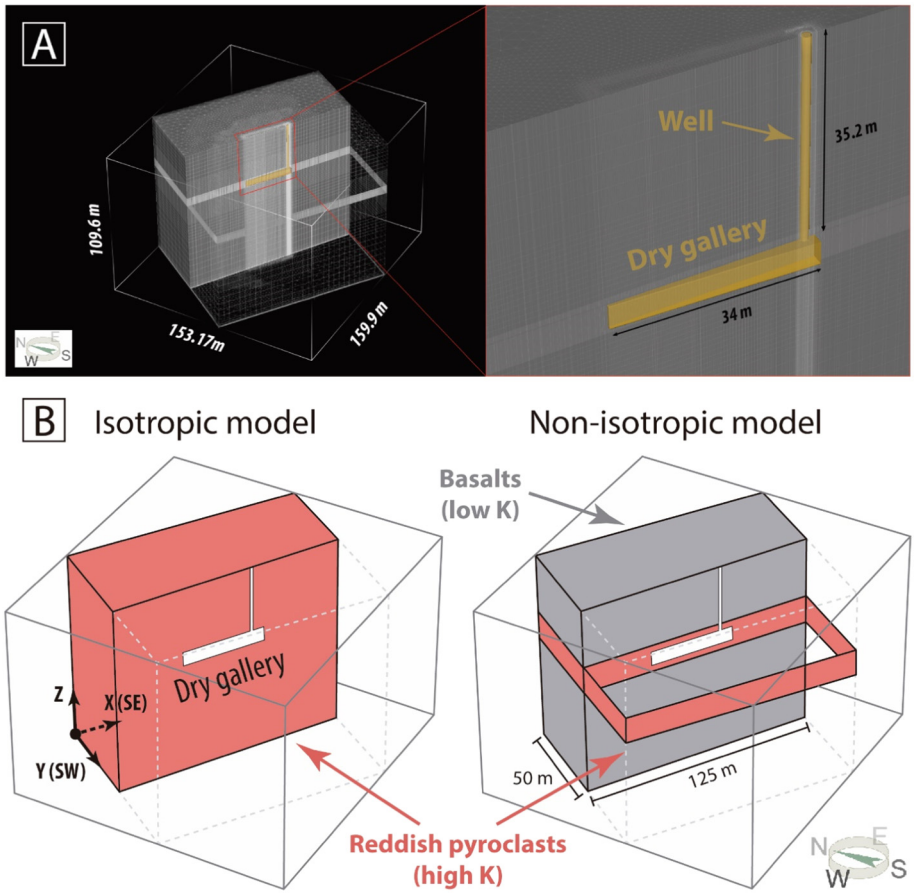

Fig. 3. Numerical model set-up. A) 3D mesh of the numerical model and location of the dry gallery system. On the right side, detailed view of the mesh around the dry gallery system (well and dry gallery). B) Isotropic (homogeneous K field of 140 m·day^{-1}) and non-isotropic (high K layer surrounded by impervious rocks) geological configurations evaluated through the 3D numerical model.

these boundaries, they did not constrain the results. For the rest of the domain, a hydraulic head of 0 m and a saturation equal to 0 was set as initial conditions. The simulated time period was one day, with a variable time step control. The time step length increased from $1{\cdot}10^{-8}$ at the beginning of the simulation to $7{\cdot}10^{-4}$ days at the end of the simulation. As stormwater needs to be infiltrated in short times, one day of simulation is considered long enough to assess the infiltration process in dry galleries.

Two simulations were performed to evaluate the infiltration process under (i) an isotropic K field (isotropic simulation) and (ii) considering the dry gallery is installed into a 6 m thick high permeability layer of reddish pyroclasts, limited to the top and bottom by impermeable volcanic rocks (non-isotropic simulation) (Fig. 3B). The isotropic simulation aimed to reproduce the infiltration from dry galleries, assuming there are no lithological constraints in terms of impermeable layers at the top and bottom. The non-isotropic simulation aimed to reproduce the wetting front propagation in the most frequent situation in volcanic aquifers, when permeable layers are intercalated between other impermeable layers. The comparison of both results, an ideal first result and a second result representing the most common case in which dry galleries are installed, allowed us to understand how to correctly assess the performance of these systems and what criteria to follow for their installation. The parametrization of the domain was carried out based on the field data of the *Santa Cruz* dry gallery (IGME, 2021). Both simulations fulfilled a K of 140 m·day^{-1} around the gallery. However, in the first simulation, this value of K was applied to the entire domain while, in the second simulation, this value of K was assigned to a layer of thickness of 6 m, coinciding with the infiltration gallery, and the rest of the domain was considered impermeable. An effective porosity of 30% was set. Using a computer with a CPU Intel® Core™ i9-10980X and 64 GB RAM, each simulation took one week to run due to the tiny time steps required to simulate such strong pressure gradients under 3D unsaturated conditions.

4. Results and discussion

4.1. Lithological constraint of the wetting front geometry and propagation velocity

Both transient simulations, the isotropic (homogenous domain of permeable reddish pyroclasts) and non-isotropic simulation (permeable reddish pyroclasts layer surrounded by impermeable basalts) started considering a hypothetical initial situation in which the dry gallery was surrounded by a completely unsaturated media and the dry gallery had a constant equivalent height of 39.2 m (taken as reference the bottom of the gallery) of water column, i.e., it was completely filled of water. After one day of simulation, the saturated bulge resulting from the wetting front advance is shown in Fig. 4.

For the first simulation, considering an isotropic variable saturated K field, the saturated bulge evolved following a close to radial pattern, with a further downward development along the z-axis (Fig. 4A) as consequence of the gravity. However, the isotropic simulation considered a highly idealized scenario, whereas the natural subsurface is inherently highly heterogeneous, especially in volcanic areas where different lava flows and volcanic rocks are stacked on top of each other. The second simulation, considering a 6 m thick layer of permeable reddish pyroclasts, showed the wetting front had a clear preference for expanding laterally along the x-y plane than along the z axis, where it was strongly constricted by impermeable rocks 1 m away (Fig. 4B). Thus, the saturated bulge resulting from infiltration in a gallery located in a permeable pyroclastic layer is, as expected,

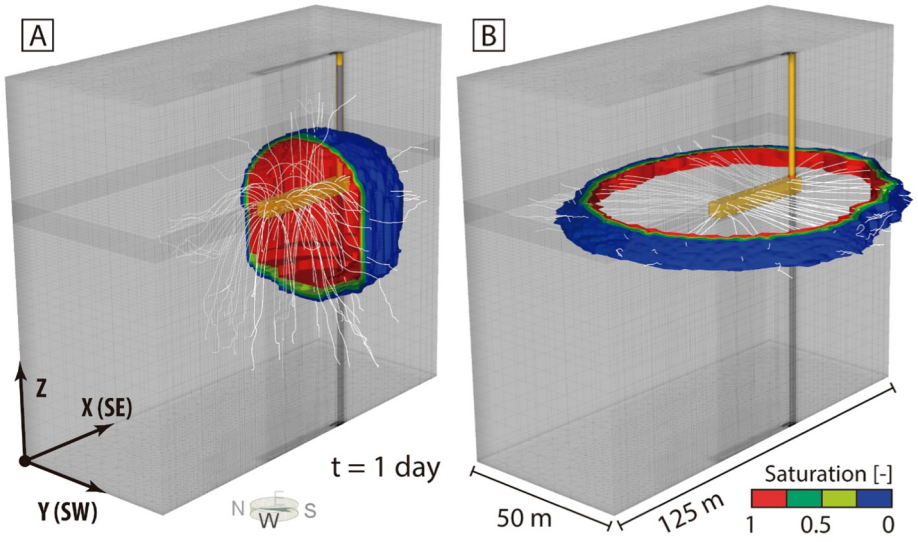

Fig. 4. 3D wetting front computed by the numerical model after one day of simulation for the isotropic (A) and non-isotropic (B) simulations. Note, in white, the flow pathlines traveling from the dry gallery toward the wetting front. Dry gallery and well are highlighted in yellow. Only half of the mesh is shown for visualization purposes.

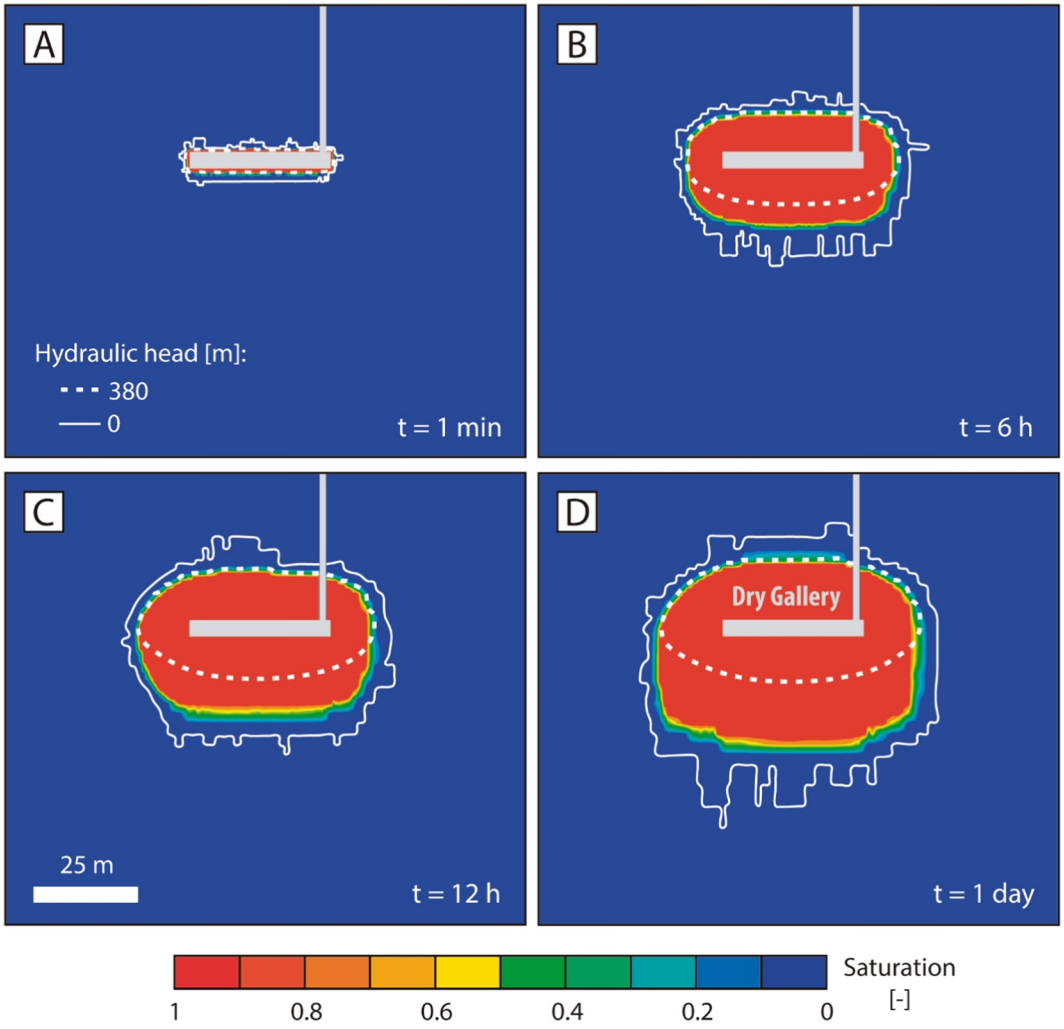

Fig. 5. Wetting front propagation resulting from the isotropic simulation at 1 min (A), 6 h (B), 12 h (C) and 1 day (D). This cross-section matches the cross-section shown in Figs. 3 and 4. Reference hydraulic head isolines of 0 and 380 m are shown to highlight the main part of the wetting front where the hydraulic gradient is higher.

characterized by a ring morphology with great lateral and no vertical development, in contrast to the relative spherical morphology with greater development in the gravitational direction expected in an isotropic media. Note that although these two simulations represent plausible situations, they represent the two extreme cases, and intermediate solutions between both cases are possible, for example, assuming a thicker permeable layer.

These two simulations demonstrated the need to evaluate the infiltration process from a transient and non-stationary approach. During the first step of both simulations, the terrain around the gallery presented negative pressures (saturation lower than 1) (Figs. 5A and 6A). In these early stages, the wetting front had a very narrow width and the entire pressure gradient is concentrated in less than 1 m. If it is taken into account that the effective K, considered as a function of soil saturation, increases with its saturation degree, it can be explained how this initial situation represents a challenge for the convergence of the numerical model solution, and long computational times were required. However, as the saturation front expanded, its thickness increased and the hydraulic gradients were attenuated and adapted to the new space generated between the infiltration gallery and the wetting front (see evolution from A to D in Figs. 5 and 6).

The distances traveled by the wetting front across the x-y plane ranged between 12.5 and 19.8 m for the isotropic simulation and between 27.4 and 41.2 m for the non-isotropic simulation (Fig. 7A). Also, the wetting front extended vertically between 14.5 m (upwards) and 26.1 m (downwards) for the isotropic simulation (the non-isotropic simulation reached the top and bottom impermeable rocks after a few steps). In all cases and directions, the fastest advance of the wetting front took place during the earliest times (<2 h), with velocities around 1000 $m{\cdot}d^{-1}$ (Fig. 7B). As time progressed, the velocity of the wetting front progressively decreased, with values around 10 $m{\cdot}d^{-1}$ after one day of simulation. The traveled distances and propagation velocities in the case of the non-isotropic simulation were higher than for the isotropic simulation at all times (Fig. 7). Highly permeable rocks (reddish pyroclasts) limited at top and bottom by impermeable rocks (basalts) enhanced the rapid movement of the wetting front in the horizontal direction and facilitated infiltration of water over a larger lateral extension. This is something that should be considered when deciding on the placement of a dry gallery installation, especially if there are infrastructures that are laterally close or there is a risk of intercepting faults that could connect different aquifer levels and then lead to a degradation of the chemistry of water. The location of a gallery in a horizontal permeable layer isolated by impervious rocks at the top and bottom reduces travel times of a potential contaminant through the x-y plane and then increases the risk of contamination laterally. However, travel times in the vertical direction are reduced, making it difficult for a potential pollutant to advance vertically and reaching other aquifers. Therefore, when dry galleries are used as a stormwater management facility, and not as a managed infiltration facility where a better infiltration water quality is usually expected, environmental impacts would be reduced if dry galleries are placed on levels where there is an impermeable layer underneath, as long as there are no sensitive infrastructures or faults that can be horizontally intercepted. However, from a production point of view, it would be necessary to analyze the effect that this enhancement of lateral propagation versus vertical downstream propagation has on infiltration rates.

4.2. Infiltration performance of dry galleries

The infiltration rates in both simulations showed a similar behavior to the propagation velocity of the wetting front. In the early stages, maximum infiltration rates above 2 $m^3{\cdot}s^{-1}$ for the isotropic case and 1.6 $m^3{\cdot}s^{-1}$ for the case that considered the installation of the gallery in a horizontal permeable layer were reached (Fig. 8). These infiltration rates were reduced to 0.25 and 0.1 $m^3{\cdot}s^{-1}$, respectively, after one day of simulation as a consequence of the reduction in the hydraulic gradient between the gallery and the aquifer over time. A trend toward a unit gradient is to be expected after several days, although probably outside the operational time range of these systems. Since storm events rarely last more than a few hours, the stormwater infiltration process should be understood as a transient process, and assuming steady-state conditions would lead to major errors as discussed below. Thus, after one day of simulation, the volume of infiltrated water for the isotropic case was $2.7{\cdot}10^4$ m^3 and for the non-isotropic case $1.15{\cdot}10^4$ m^3. Clogging and other physical malfunctions described for other infiltration facilities used for extended periods of time (Bouwer, 2002; Gonzalez-Merchan et al., 2012; Le Coustumer and Barraud, 2007; Pavelic et al., 2007; Siriwardene et al., 2007) should be assessed for dry galleries in future studies.

The geological constraint in the advance of the wetting front along the z-axis led to a decrease in the infiltration rate of more than 50% after one

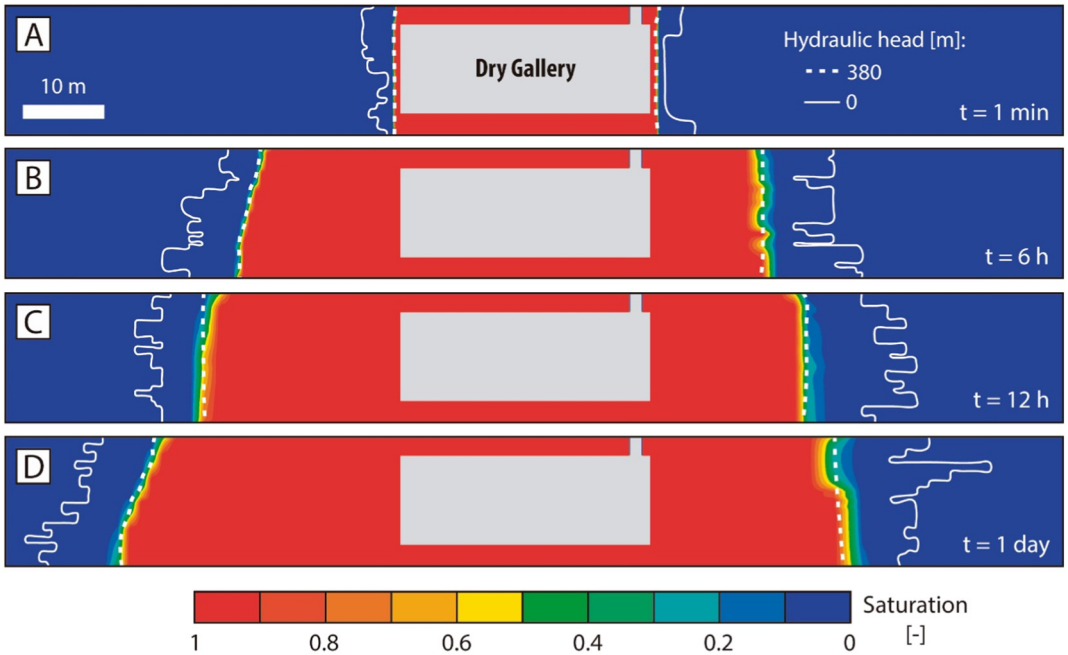

Fig. 6. Wetting front propagation resulting from the non-isotropic simulation at 1 min (A), 6 h (B), 12 h (C) and 1 day (D). This cross-section matches the cross-section shown in Figs. 3 and 4. Reference hydraulic head isolines of 0 and 380 m are shown to highlight the main part of the wetting front where the hydraulic gradient is higher. The vertical scale was increased by three and only permeable layer of reddish pyroclasts was shown as the overlying and underlying rocks are impermeable.

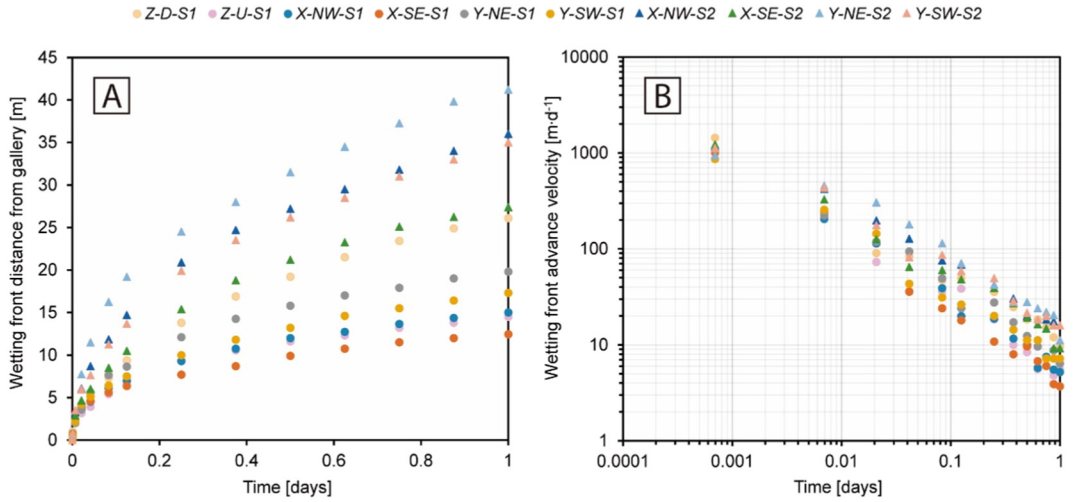

Fig. 7. A) Wetting front distance measured from the dry gallery over one day of simulation for the isotropic (dots) and non-isotropic (triangles) geological configurations (see Fig. 3B). The saturation isosurface of 0.5 was taken as reference for measurement. Labels show the axis component (X, Y, Z) in the first term, the measurement direction from the dry gallery along each axis (NW, SE, NE, SW, U-upward and D-downward) in the second term and the model simulation (S1, isotropic configuration; S2, non-isotropic configuration) in the third term. See Figs. 2–4 for a precise orientation of the dry gallery system. B) Velocities resulting for the wetting front propagation.

day of infiltration (Fig. 8). Therefore, it is clear that the layering of the volcanic rocks strongly conditions the infiltration rate from dry galleries and cannot be neglected. Although greater lateral versus vertical expansion can often be beneficial in protecting underlying aquifers from contamination, from a performance standpoint it is counterproductive. This is where the purpose of the dry gallery (managed recharge of aquifers versus stormwater management) and the risk-benefit analysis for each specific facility comes into play. In many cases, intermediate geological situations with permeable layers of greater thickness than the one considered in this work can allow isolation of the lower aquifers from the infiltrated water without suffering very marked reductions in the infiltration rate and facilitate decision-making based on the results presented in this study for the two extreme cases.

4.3. Neglecting unsaturated conditions leads to undersizing the dry galleries

The error made by neglecting the negative pressures and strong hydraulic gradients associated with the unsaturated zone, which means considering just a unit gradient between the gallery and the aquifer, was computed in Fig. 9. Assuming Darcy's law ($Q = K \cdot A \cdot i$ where A is the area and i the hydraulic gradient) with a saturated K of 140 $m \cdot d^{-1}$ and an infiltration surface area of 595 m^2, the estimated infiltration of the *Santa Cruz* dry gallery would be 0.96 $m^3 \cdot s^{-1}$. According to the model results (Fig. 8), the infiltration rates during the first 3 min were about twice (2 and 1.6 $m^3 \cdot s^{-1}$ for the isotropic and non-isotropic simulation, respectively) the estimated infiltration rate neglecting unsaturated conditions (0.96 $m^3 \cdot s^{-1}$). However, after 3 min, the simulated infiltration rates dropped below this

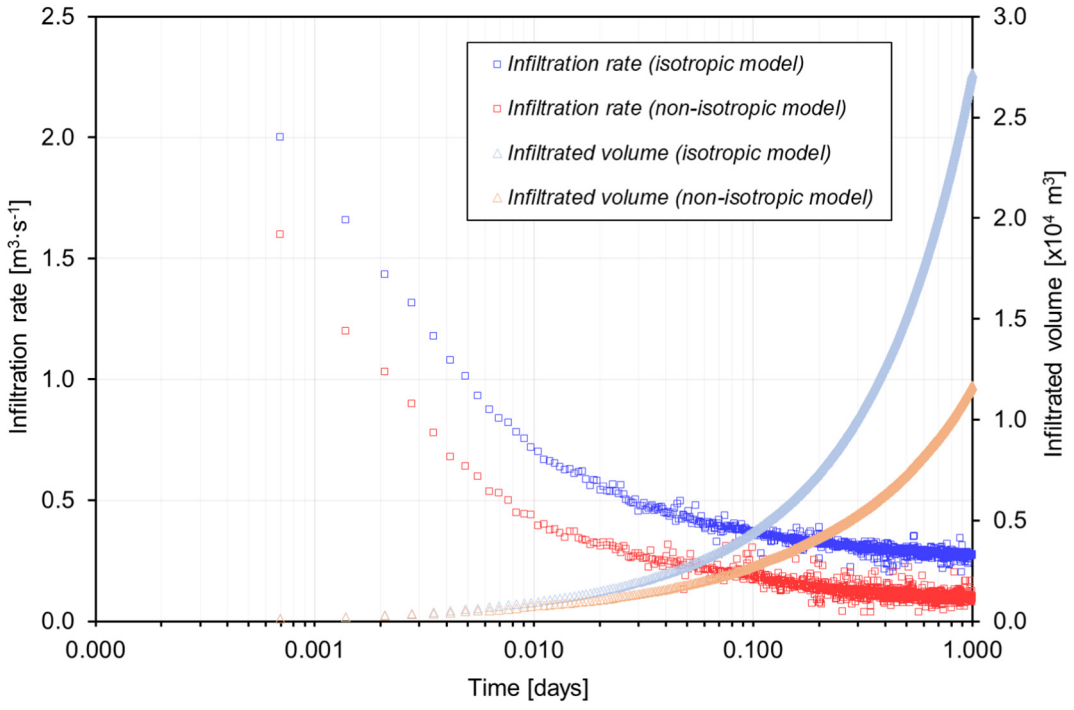

Fig. 8. Computed infiltration rate and infiltration volume over time for the isotropic and non-isotropic geological configurations.

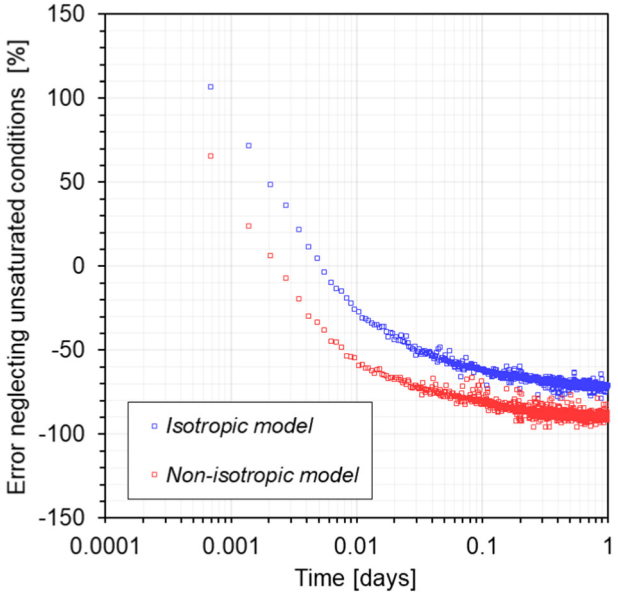

Fig. 9. Error committed in the infiltration rate calculation by neglecting unsaturated conditions. Errors for both geological configurations (isotropic and non-isotropic) are displayed. Errors below 0% lead to underestimating the size of the dry gallery due to overestimation of the infiltration rate.

reference value. This led to errors by underestimation of the infiltration capacity of more than 100% during the first 3 min of injection. However, these initial underestimation errors evolved to an overestimation error of the infiltration rate after less than 5 min and for the rest of the simulation time. In addition, these overestimation errors progressively increased until they were close to 100%, after one day of simulation. The error made by overestimating the infiltration rate leads to undersizing the dry gallery.

5. Conclusions

The first numerical modeling study of a dry gallery stormwater infiltration facility has allowed us to (i) explain the complex geometry and movement of the wetting front in homogeneous and layered hydraulic conductivity (K) fields, (ii) estimate wetting front propagation velocities and travel times for potential infiltrated contaminants, (iii) evaluate the better location of these facilities to avoid environmental impacts, (iv) assess infiltration performance of dry galleries, and (v) quantify the errors made in dry gallery sizing by neglecting unsaturated conditions.

Numerical modeling confirmed that the layered structure of the volcanic rocks strongly conditions the infiltration pattern from dry galleries and, therefore, it should be considered for the design and management of dry galleries and other stormwater infiltration facilities globally. Since storm events rarely last more than a few hours, the stormwater infiltration process should be understood as a transient process. The fastest advance of the wetting front and the highest infiltration rate took place during the earliest times of infiltration (<2 h), with propagation velocities above 1000 $m{\cdot}d^{-1}$ and infiltration rates between 2 and 1.6 $m^3{\cdot}s^{-1}$ for the isotropic and non-isotropic simulations, respectively. After one day of infiltration, as a consequence of the hydraulic gradient attenuation, the propagation velocity of the wetting front decreased to 10 $m{\cdot}d^{-1}$ and the infiltration rate to 0.25 $m^3{\cdot}s^{-1}$ for the homogenous configuration and 0.1 $m^3{\cdot}s^{-1}$ for the layered configuration. Neglecting unsaturated conditions leads to dry gallery sizing errors of 100% by underestimation. In addition, when the impermeable bottom is too close to the gallery, the infiltration performance of the dry gallery can be significantly reduced (>50%) because gravity favors infiltration downwards.

Stormwater management is a global problem and, due to climate change, frequency and intensity will increase. Dry galleries could help to better manage stormwater events, prevent or mitigate floods, and increase groundwater storage by artificial recharge, which is benign in preventing seawater intrusion. This is of utmost importance, especially for islands in dry regions and with increasing water scarcity. The proposed design criteria for dry galleries in our work might help to use this concept in other places with a similar climatic and hydrogeological conditions.

CRediT authorship contribution statement

Marazuela, M.A.: Conceptualization, Methodology, Investigation, Writing - Original Draft, Visualization, Formal analysis.

García-Gil, A.: Conceptualization, Methodology, Investigation, Writing - Review & Editing, Funding acquisition.

Santamarta, J.C.: Writing - Review & Editing.

Gasco-Cavero, S.: Writing - Review & Editing.

Cruz-Pérez, N.: Writing - Review & Editing.

Hofmann, T.: Writing - Review & Editing.

Declaration of competing interest

Alejandro Garcia Gil reports financial support was provided by Government of Spain. Alejandro Garcia Gil reports financial support was provided by European Union.

Acknowledgments

This research was partially supported by the Spanish Research Agency (project SAGE4CAN PID2020-114218RA-100), and European Union's Horizon 2020 research and innovation programme under grant agreement 101037424, project ARSINOE (Climate resilient regions through systemic solutions and innovations). The authors thank Jesús Mateo Lázaro and three anonymous reviewers for timely and constructive feedback that improved the quality of this manuscript. M. Á. Marazuela acknowledges DHI for sponsoring the FEFLOW license.

References

Akan, A.O., 2002. Sizing stormwater infiltration structures. J. Hydraul. Eng. 128, 534–537. https://doi.org/10.1061/(asce)0733-9429(2002)128:5(534).

Allen, M.R., Ingram, W.J., 2002. Constraints on future changes in climate and the hydrologic cycle. Nature 419, 228–232. https://doi.org/10.1038/nature01092.

Anguita, F., Hernán, F., 2000. The Canary Islands origin: a unifying model. J. Volcanol. Geotherm. Res. 103, 1–26. https://doi.org/10.1016/S0377-0273(00)00195-5.

Barraud, S., Gautier, A., Bardin, J.P., Riou, V., 1999. The impact of intentional stormwater infiltration on soil and groundwater. Water Sci. Technol. 39, 185–192. https://doi.org/10.1016/S0273-1223(99)00022-0.

Bekele, E., Toze, S., Patterson, B., Fegg, W., Shackleton, M., Higginson, S., 2013. Evaluating two infiltration gallery designs for managed aquifer recharge using secondary treated wastewater. J. Environ. Manag. 117, 115–120. https://doi.org/10.1016/j.jenvman.2012.12.018.

Berg, P., Moseley, C., Haerter, J.O., 2013. Strong increase in convective precipitation in response to higher temperatures. Nat. Geosci. 6, 181–185. https://doi.org/10.1038/ngeo1731.

Bouwer, H., 2002. Artificial recharge of groundwater: hydrogeology and engineering. Hydrogeol. J. 10, 121–142. https://doi.org/10.1007/s10040-001-0182-4.

Clark, S.E., Pitt, R., 2007. Influencing factors and a proposed evaluation methodology for predicting groundwater contamination potential from stormwater infiltration activities. Water Environ. Res. 79, 29–36. https://doi.org/10.2175/106143006x143173.

Custodio, E., Guerra, J.A., Jiménez, J., Medina, J.A., Soler, C., 1983. The effects of agriculture on the volcanic aquifers of the Canary Islands. Environ. Geol. 5, 225–231. https://doi.org/10.1007/BF02414868.

Custodio, E., Cabrera, M.del C., Poncela, R., Cruz-Fuentes, T., Naranjo, G., de Miguel, L.O.P., 2015. Comments on uncertainty in groundwater governance in the volcanic Canary Islands, Spain. Water (Switzerland) 7, 2952–2970. https://doi.org/10.3390/w7062952.

Custodio, E., Cabrera, M.del C., Poncela, R., Puga, L.O., Skupien, E., del Villar, A., 2016. Groundwater intensive exploitation and mining in Gran Canaria and Tenerife, Canary Islands, Spain: hydrogeological, environmental, economic and social aspects. Sci. Total Environ. 557–558, 425–437. https://doi.org/10.1016/j.scitotenv.2016.03.038.

Dallman, S., Spongberg, M., 2012. Expanding local water supplies: assessing the impacts of stormwater infiltration on groundwater quality. Prof. Geogr. 64, 232–249. https://doi.org/10.1080/00330124.2011.600226.

Dezert, T., Fargier, Y., Palma Lopes, S., Côte, P., 2019. Geophysical and geotechnical methods for fluvial levee investigation: a review. Eng. Geol. 260, 105206. https://doi.org/10.1016/j.enggeo.2019.105206.

Diersch, H.-J.G., 2014. FEFLOW: Finite Element Modeling of Flow, Mass And Heat Transport in Porous And Fractured Media. Springer-Verlag, Berlin Heidelberg https://doi.org/10.1007/978-3-642-38739-5.

Dillon, P., 2005. Future management of aquifer recharge. Hydrogeol. J. 13, 313–316. https://doi.org/10.1007/s10040-004-0413-6.

Edwards, E.C., Harter, T., Fogg, G.E., Washburn, B., Hamad, H., 2016. Assessing the effectiveness of drywells as tools for stormwater management and aquifer recharge and their groundwater contamination potential. J. Hydrol. 539, 539–553. https://doi.org/10.1016/j.jhydrol.2016.05.059.

Elrick, D., Reynolds, W., Tan, K., 1989. Hydraulic conductivity measurements in the unsaturated zone using improved well analyses. Groundw. Monit. Remediat. 9, 184–193. https://doi.org/10.1111/j.1745-6592.1989.tb01162.x.

Fischer, E.M., Knutti, R., 2015. Anthropogenic contribution to global occurrence of heavy-precipitation and high-temperature extremes. Nat. Clim. Chang. 5, 560–564. https://doi.org/10.1038/nclimate2617.

Fischer, E.M., Knutti, R., 2016. Observed heavy precipitation increase confirms theory and early models. Nat. Clim. Chang. 6, 986–991. https://doi.org/10.1038/nclimate3110.

Folch, A., del Val, L., Luquot, L., Martínez-Pérez, L., Bellmunt, F., Le Lay, H., Rodellas, V., Ferrer, N., Palacios, A., Fernández, S., Marazuela, M.A., Diego-Feliu, M., Pool, M., Goyetche, T., Ledo, J., Pezard, P., Bour, O., Queralt, P., Marcuello, A., Garcia-Orellana, J., Saaltink, M.W., Vázquez-Suñé, E., Carrera, J., 2020. Combining fiber optic DTS, cross-hole ERT and time-lapse induction logging to characterize and monitor a coastal aquifer. J. Hydrol. 588, 125050. https://doi.org/10.1016/j.jhydrol.2020.125050.

van Genuchten, M.T., 1980. A closed-form equation for predicting the hydraulic conductivity of unsaturated soils. Soil Sci. Soc. Am. J. 44, 892–898. https://doi.org/10.2136/sssaj1980.03615995004400050002x.

Gonzalez-Merchan, C., Barraud, S., Coustumer, S.Le, Fletcher, T., 2012. Monitoring of clogging evolution in the stormwater infiltration system and determinant factors. Eur. J. Environ. Civ. Eng. 16, s34–s47. https://doi.org/10.1080/19648189.2012.682457.

Gössling, S., 2001. The consequences of tourism for sustainable water use on a tropical island: Zanzibar,Tanzania. J. Environ. Manag. 61, 179–191. https://doi.org/10.1006/jema.2000.0403.

Gray, W.G., Hassanizadeh, S.M., 1991a. Paradoxes and realities in unsaturated flow theory. Water Resour. Res. 27, 1847–1854. https://doi.org/10.1029/91WR01259.

Gray, W.G., Hassanizadeh, S.M., 1991b. Unsaturated flow theory including interfacial phenomena. Water Resour. Res. 27, 1855–1863. https://doi.org/10.1029/91WR01260.

Hernández-Martín, R., Antonova, N., Celis-Sosa, D., Fernández-Hernández, C., González-Hernández, M., Mendoza-Jimenez, J., Padrón-Fumero, N., Rodríguez-González, P., Santana-Talavera, A., Simancas-Cruz, M., 2021. Tourism Observatory of the Canary Islands. https://doi.org/10.25145/b.TourismCanary.2021.

Herrera, P.A., Marazuela, M.A., Hofmann, T., 2022. Parameter estimation and uncertainty analysis in hydrological modeling. WIREs Water 9, e1569. https://doi.org/10.1002/wat2.1569.

IGME, 2021. Informe en materia de la viabilidad técnica y administrativa de evacuar al subsuelo el agua procedente de redes de pluviales, demarcación hidrográfica de Tenerife.

Izuka, S.K., 2011. Potential effects of roadside dry wells on groundwater quality on the island of Hawai'i — assessment using numerical groundwater models. Scientific Investigations Report, pp. 2011–5072.

Kindred, J.S., Reynolds, W.D., 2020. Using the borehole permeameter to estimate saturated hydraulic conductivity for glacially over-consolidated soils. Hydrogeol. J. 28, 1909–1924. https://doi.org/10.1007/s10040-020-02149-3.

Kool, J.B., Parker, J.C., van Genuchten, M.T., 1987. Parameter estimation for unsaturated flow and transport models - a review. J. Hydrol. 91, 255–293. https://doi.org/10.1016/0022-1694(87)90207-1.

Le Coustumer, S., Barraud, S., 2007. Long-term hydraulic and pollution retention performance of infiltration systems. Water Sci. Technol. 55, 235–243. https://doi.org/10.2166/wst.2007.114.

Lefranc, E., 1936. Procédé de mesure de la perméabilité des sols dans les nappes aquifères et application au calcul du débit des puits. Le Génie Civ. 109, pp. 306–308.

Lefranc, E., 1937. La théorie des poches absorbantes et son application à la détermination du coefficient de perméabilité en place et au calcul du débit des nappes d'eau. Le Génie Civ. 111, pp. 409–413.

Luijendijk, E., Gleeson, T., Moosdorf, N., 2020. Fresh groundwater discharge insignificant for the world's oceans but important for coastal ecosystems. Nat. Commun. 11, 1260. https://doi.org/10.1038/s41467-020-15064-8.

Marazuela, M.A., Vázquez-Suñé, E., Custodio, E., Palma, T., García-Gil, A., Ayora, C., 2018. 3D mapping, hydrodynamics and modelling of the freshwater-brine mixing zone in salt flats similar to the Salar de Atacama (Chile). J. Hydrol. 561, 223–235. https://doi.org/10.1016/j.jhydrol.2018.04.010.

Marrero-Diaz, R., Alcalá, F.J., Pérez, N.M., López, D.L., Melián, G.V., Padrón, E., Padilla, G.D., 2015. Aquifer recharge estimation through atmospheric chloride mass balance at Las Cañadas Caldera, Tenerife, Canary Islands, Spain. Water (Switzerland) 7, 2451–2471. https://doi.org/10.3390/w7052451.

Martínez-Pérez, L., Luquot, L., Carrera, J., Marazuela, M.A., Goyetche, T., Pool, M., Palacios, A., Bellmunt, F., Ledo, J., Ferrer, N., del Val, L., Pezard, P.A., García-Orellana, J., Diego-Feliu, M., Rodellas, V., Saaltink, M.W., Vázquez-Suñé, E., Folch, A., 2022. A multidisciplinary approach to characterizing coastal alluvial aquifers to improve understanding of seawater intrusion and submarine groundwater discharge. J. Hydrol. 127510. https://doi.org/10.1016/j.jhydrol.2022.127510.

Massmann, J., 2004. An Approach for Estimating Infiltration Rates for Stormwater Infiltration Dry Wells.

Myhre, G., Alterskjær, K., Stjern, C.W., Hodnebrog, Ø., Marelle, L., Samset, B.H., Sillmann, J., Schaller, N., Fischer, E., Schulz, M., Stohl, A., 2019. Frequency of extreme precipitation increases extensively with event rareness under global warming. Sci. Rep. 9, 16063. https://doi.org/10.1038/s41598-019-52277-4.

Papapostolou, C.M., Kondili, E.M., Zafirakis, D.P., Tzanes, G.T., 2020. Sustainable water supply systems for the islands: the integration with the energy problem. Renew. Energy 146, 2577–2588. https://doi.org/10.1016/j.renene.2019.07.130.

Pavelic, P., Dillon, P.J., Barry, K.E., Vanderzalm, J.L., Correll, R.L., Rinck-Pfeiffer, S.M., 2007. Water quality effects on clogging rates during reclaimed water ASR in a carbonate aquifer. J. Hydrol. 334, 1–16. https://doi.org/10.1016/j.jhydrol.2006.08.009.

Pfahl, S., O'Gorman, P.A., Fischer, E.M., 2017. Understanding the regional pattern of projected future changes in extreme precipitation. Nat. Clim. Chang. 7, 423–427. https://doi.org/10.1038/nclimate3287.

Santamarta-Cerezal, J.C., Cabrera Santana, M.C., Custodio, E., Delgado Díaz, S.N., González González, J.J., Hardisson de la Torre, A., Hernández Gutiérrez, L.E., Hernández Sánchez, C., Jiménez Mendoza, C.C., Neris Tomé, J., Rodríguez Losada, J.A., Santana Pérez, L.M., Suárez Moreno, F., Suárez Pérez, A., Tejedor Salguero, M., 2013. Hidrología y recursos hídricos en islas y terrenos volcánicos: Métodos, Técnicas y Experiencias en las Islas Canarias. College of Forestry Engineers, Madrid.

Sasidharan, S., Bradford, S.A., Šimůnek, J., DeJong, B., Kraemer, S.R., 2018. Evaluating drywells for stormwater management and enhanced aquifer recharge. Adv. Water Resour. 116, 167–177. https://doi.org/10.1016/j.advwatres.2018.04.003.

Sasidharan, S., Bradford, S.A., Šimůnek, J., Kraemer, S.R., 2019. Drywell infiltration and hydraulic properties in heterogeneous soil profiles. J. Hydrol. 570, 598–611. https://doi.org/10.1016/j.jhydrol.2018.12.073.

Siriwardene, N.R., Deletic, A., Fletcher, T.D., 2007. Clogging of stormwater gravel infiltration systems and filters: insights from a laboratory study. Water Res. 41, 1433–1440. https://doi.org/10.1016/j.watres.2006.12.040.

Stephens, D.B., 1979. Analysis of Constant Head Borehole Infiltration Tests in the Vadose Zone. The University of Arizona.

Stephens, D.B., 1992. Application of the borehole permeameter. Advances in Measurement of Soil Physical Properties: Bringing Theory Into Practice. Soil Science Society of America, p. 288.

Stephens, D.B., 1996. Vadose Zone Hydrology. CRC Press.

Stephens, D.B., Lambert, K., Watson, D., 1987. Regression models for hydraulic conductivity and field test of the borehole permeameter. Water Resour. Res. 23, 2207–2214. https://doi.org/10.1029/WR023i012p02207.

Vázquez-Suñé, E., Marazuela, M.Á., Velasco, V., Diviu, M., Pérez-Estaún, A., Álvarez-Marrón, J., 2016. A geological model for the management of subsurface data in the urban environment of Barcelona and surrounding area. Solid Earth 7. https://doi.org/10.5194/se-7-1317-2016.

Zhang, H., Xu, Y., Kanyerere, T., 2020. A review of the managed aquifer recharge: historical development, current situation and perspectives. Phys. Chem. Earth 118–119, 102887. https://doi.org/10.1016/j.pce.2020.102887.